The influence of soft tissue artifacts on multi-segment foot kinematics

Schallig, Wouter; Streekstra, Geert J.; Hulshof, Chantal M.; Kleipool, Roeland P.; Dobbe, Johannes G.G.; Maas, Mario; Harlaar, Jaap; van der Krogt, Marjolein M.; van den Noort, Josien C.

DOI
10.1016/j.jbiomech.2021.110359

Publication date
2021

Document Version
Final published version

Published in
Journal of Biomechanics

Journal of Biomechanics 120 (2021) 110359

Contents lists available at ScienceDirect

Journal of Biomechanics

journal homepage: www.elsevier.com/locate/jbiomech
www.JBiomech.com

The influence of soft tissue artifacts on multi-segment foot kinematics

Wouter Schallig [a,b,*], Geert J. Streekstra [b,c], Chantal M. Hulshof [a], Roeland P. Kleipool [d], Johannes G.G. Dobbe [c], Mario Maas [b], Jaap Harlaar [a,e], Marjolein M. van der Krogt [a], Josien C. van den Noort [a,b]

[a] Amsterdam UMC, Vrije Universiteit Amsterdam, Rehabilitation Medicine, Amsterdam Movement Sciences, de Boelelaan 1117, Amsterdam, the Netherlands
[b] Amsterdam UMC, University of Amsterdam, Radiology and Nuclear Medicine, Medical Imaging Quantification Center (MIQC), Amsterdam Movement Sciences, Meibergdreef 9, Amsterdam, the Netherlands
[c] Amsterdam UMC, University of Amsterdam, Biomedical Engineering and Physics, Amsterdam Movement Sciences, Meibergdreef 9, Amsterdam, the Netherlands
[d] Amsterdam UMC, University of Amsterdam, Medical Biology, Amsterdam Movement Sciences, Meibergdreef 9, Amsterdam, the Netherlands
[e] Department of Biomechanical Engineering, Delft University of Technology, Delft, the Netherlands

ARTICLE INFO

Article history:
Accepted 22 February 2021

Keywords:
Foot kinematics
Gait analysis
Skin motion artifact
Measurement error
Computed tomography

ABSTRACT

Movement of skin markers with respect to their underlying bone (i.e. soft tissue artifacts (STAs)) might corrupt the accuracy of marker-based movement analyses. This study aims to quantify STAs in 3D for foot markers and their effect on multi-segment foot kinematics as calculated by the Oxford and Rizzoli Foot Models (OFM, RFM). Fifteen subjects with asymptomatic feet were seated on a custom-made loading device on a computed tomography (CT) table, with a combined OFM and RFM marker set on their right foot. One unloaded reference CT-scan with neutral foot position was performed, followed by 9 loaded CT-scans at different foot positions. The 3D-displacement (i.e. STA) of each marker in the underlying bone coordinate system between the reference scan and other scans was calculated. Subsequently, segment orientations and joint angles were calculated from the marker positions according to OFM and RFM definitions with and without STAs. The differences in degrees were defined as the errors caused by the marker displacements. Markers on the lateral malleolus and proximally on the posterior aspect of the calcaneus showed the largest STAs. The hindfoot-shank joint angle was most affected by STAs in the most extreme foot position (40° plantar flexion) in the sagittal plane for RFM (mean: 6.7°, max: 11.8°) and the transverse plane for OFM (mean: 3.9°, max: 6.8°). This study showed that STAs introduce clinically relevant errors in multi-segment foot kinematics. Moreover, it identified marker locations that are most affected by STAs, suggesting that their use within multi-segment foot models should be reconsidered.

1. Introduction

Skin-mounted marker-based multi-segment foot models are frequently used to measure foot kinematics during gait, for instance to assess foot and ankle problems in patient populations. Many different multi-segment foot models have been proposed, of which the Oxford Foot Model (OFM) and Rizzoli Foot Model (RFM) have been used most frequently (Leardini et al., 2019). OFM and RFM provide a different kinematic output when measuring the same gait trial (Schallig et al., 2020). However, it is unclear how accurate each of these models are, which is especially of importance when the data is used for clinical decision-making.

Soft Tissue Artifacts (STAs) are a well-known source of error in marker-based human motion analyses, affecting the accuracy of kinematic measurements (Leardini et al., 2005). Skin-mounted markers are placed to represent underlying anatomical bony landmarks. However, when motions like gait are performed, soft tissue displacement causes relative motion between a marker and its corresponding bone, thereby affecting the derived kinematics. Especially for markers on the foot, STAs have the potential to influence the measured kinematics significantly. The inter-marker distances are small, hence a displacement causes relatively large angular errors compared to markers that are further apart.

Literature shows that STAs of markers on the foot are substantial and variable across subjects and marker locations (Birch and Deschamps, 2011; Chen et al., 2011; Kessler et al., 2019; Maslen and Ackland, 1994; Nester et al., 2007; Okita et al., 2009; Reinschmidt et al., 1997; Shultz et al., 2011; Tranberg and Karlsson, 1998; Westblad et al., 2002). Intra-cortical percutaneous pins with markers have been used previously to compare the

* Corresponding author at: Amsterdam UMC, Vrije Universiteit Amsterdam, Department of Rehabilitation Medicine, Amsterdam Movement Sciences, De Boelelaan 1117, 1081 HV Amsterdam, The Netherlands.
E-mail address: w.schallig@amsterdamumc.nl (W. Schallig).

https://doi.org/10.1016/j.jbiomech.2021.110359
0021-9290/

motion of skin-mounted markers with respect to bone movement, which showed kinematic differences in all three anatomical planes (Nester et al., 2007; Reinschmidt et al., 1997; Westblad et al., 2002). Moreover, in 86% of all the measured kinematic data, the maximum angular difference between measuring with skin-mounted markers or bone pins was larger than 5° (Nester et al., 2007). Although bone pins do not systematically alter the gait pattern (Maiwald et al., 2017), separate trials had to be performed with markers and bone pins in most of these studies, and the bone pins might vibrate or bend during testing which introduces errors (Ramsey et al., 2003). STAs have also been quantified using imaging techniques like 2D radiographs (Birch and Deschamps, 2011; Maslen and Ackland, 1994; Tranberg and Karlsson, 1998), single plane fluoroscopy (Shultz et al., 2011) and bi-planar video radiography (Kessler et al., 2019). With these techniques, marker displacements varying from 1 to 22 mm were reported (Birch and Deschamps, 2011; Kessler et al., 2019; Shultz et al., 2011), with the highest values for the talar heads, the lateral malleolus marker (Birch and Deschamps, 2011) and the navicular marker (Shultz et al., 2011). Angular measurements have shown to be mainly affected by STAs in the frontal and transverse plane (~5°) (Birch and Deschamps, 2011; Kessler et al., 2019).

The aforementioned studies certainly provide insight into STAs of markers on the foot. However, only some of the markers of the most frequently-used multi-segment foot models (i.e. OFM and RFM) were used and part of the imaging studies only provided STAs in 2D, which is obviously limited information compared to 3D. Moreover, to our knowledge, the effect of STAs on the kinematics as calculated by OFM and RFM is unknown.

Therefore, the aim of this study is to quantify the 3D-displacements of all OFM and RFM foot markers with respect to their corresponding bones in different foot positions, and to quantify the effect of these displacements on the multi-segment foot kinematics as calculated by these foot models.

2. Methods

2.1. Subjects

Fifteen healthy subjects with an asymptomatic right foot and ankle were recruited for this study (8 females, age: 24.9 ± 1.8 years, height: 176.7 ± 7.5 cm, weight: 73.2 ± 12.1 kg). A variety of foot sizes were included (EU foot size: 40.9 ± 2.2, range: 37–44). Subjects were excluded if they 1) were pregnant, 2) wore insoles, 3) had any foot or ankle complaints in the last 3 months that could affect the gait pattern or 4) had a history of a severe trauma or surgery on the right foot. All subjects signed informed consent. Ethical approval was provided by the local medical ethics committee (registration number: NL66940.018.18).

2.2. Data collection

Twenty-four reflective spherical markers (ø9.5 mm) were placed on the right foot of each subject. These markers are normally used during 3D gait analyses with a Vicon system (Vicon Motion Systems, Ltd., Oxford, UK). Markers were placed according to OFM (Stebbins et al., 2006) and RFM (Leardini et al., 2007; Portinaro et al., 2014) definitions and additionally on the base and head of the 3rd and 4th metatarsal (Table 1, Fig. 1). The OFM marker in between the 2nd and 3rd metatarsal head could not be placed because of its proximity to other markers. Therefore, the marker on the 2nd metatarsal head was used for the OFM calculations.

Subjects were seated on a custom-made loading device (Kleipool et al., 2019) (Fig. 2A) on a computed tomography (CT) table (Brilliance 64 CT scanner, Philips Medical Systems, Best, the Netherlands). Subjects were asked to place their right foot at a movable footplate and to extend their knee. A digital spring balance (Type HCB200K500, KERN & SOHN GmbH, Balingen, Germany) was attached to a cord in between the footplate and frame to measure the force applied to the plate. The length of the cord was adjusted until the desired force of 70% of body weight (BW) was reached, which was more than sufficient to simulate weight-bearing (Kang et al., 2017). The spring balance was visible for the subject to provide feedback, since the subject was asked to keep the force constant at 70% BW by pushing the footplate.

In total, ten CT scans of the right foot were made (Table 2). All scans were made with a field of view from the bottom of the foot plate to around 10 cm above the malleoli, with a voxel size of 0.3 × 0.3 × 0.3 mm, 0.67 mm slice thickness, 0.3 mm increment, and 120 kV tube voltage. The first scan was performed with a tube charge of 50 mAs, followed by 9 low-dose scans with a tube charge of 20 mAs, to reduce radiation dose while maintaining sufficient precision (Schallig et al., 2019).

The first scan was performed unloaded (<10 N) with a neutral foot position (i.e. 0° ankle dorsiflexion). The other scans were acquired under the aforementioned load of 70% BW. In these scans the foot plate was placed in 7 different positions using wedges, ranging from 20° dorsal flexion to 40° plantar flexion and from 10° inversion to 10° eversion (Fig. 2B–C, Table 2). These values were chosen since they contain the range of motion of a healthy ankle and also represent values seen in pathological gait like cerebral palsy (Rodda et al., 2004). During one scan (TOE) the subject was asked to push away the foot plate with the forefoot, thereby simulating push-off during gait. Furthermore, for every subject two of the three most extreme foot positions (i.e. 40PF, 20DF, TOE) were randomly chosen and scanned twice to evaluate the repeatability of the measurements in our setup (results shown in Appendix A).

2.3. Data processing

The scans were processed with custom-made software (Dobbe et al., 2019). In the first scan, with the foot in neutral unloaded position, a segmentation was performed of all 24 markers and underlying 10 bones. The segmentation provided a geometrical model of the marker or bone, containing its position (i.e. centroid of the object) and for the bones also their orientation (based on the principal axes of inertia) in the coordinate system (CS) of the scanner. The segmented marker and bone objects were subsequently registered (i.e. matched) to all other scans, which provided their new position and orientation in these scans. A detailed description of the segmentation and registration procedures has been published previously (Dobbe et al., 2019; Schallig et al., 2019). For all scans, marker positions and bone positions and orientations were expressed in the global CS (i.e. scanner CS).

2.4. Data analysis

Three outcome variables were quantified: 1) the 3D marker displacement with respect to the underlying bone (i.e. STA); 2) the error in segment orientation of each foot segment due to STAs; and 3) the error in joint angles due to STAs (Fig. 3). Data was analyzed using Matlab (R2017b, MathWorks, USA).

First, 3D Marker displacement in mm was quantified for every marker with respect to its underlying bone. Marker positions were expressed in the CS of their underlying bone (Table 1), which was based on the bones' axes of inertia, by multiplying the marker position vectors in the global CS with a transformation matrix that described the bone CS in the global CS. The neutral unloaded scan was used as reference scan in which STAs were considered zero.

Table 1
Overview of the used markers.

Segment	Bone	Marker Location	Abbreviation	OFM	RFM
Shank	Tibia	Anterior aspect of tibia crest ±10 cm proximal malleolus	ASHN	X*	X*
		Most medial aspect of the medial malleolus	MMAL	X	X
	Fibula	Lateral aspect of the fibula ±10 cm proximal of malleolus	LSHN	X*	X*
		Most lateral aspect of the lateral malleolus	LMAL	X	X
Hindfoot	Calcaneus	Posterior aspect of calcaneus distal	CALD	X	X
		Posterior aspect calcaneus proximal	CALP	X	X
		Medial aspect of calcaneus, same distance from CALD as LCAL	MCAL	X	
		Lateral aspect of calcaneus, same distance from CALD as MCAL	LCAL	X	
		Peroneal tubercle	PT		X
		Sustentaculum tali	ST		X
Midfoot	Navicular	Most medial apex of navicular tuberosity	TN		X
Forefoot	Metatarsal 1	Head metatarsal 1	HM1		X
		Head metatarsal 1 medial side	HM1M	X	
		Base metatarsal 1	BM1	X	X
	Metatarsal 2	Head metatarsal 2	HM2	X#	X
		Base metatarsal 2	BM2		X
	Metatarsal 3	Head metatarsal 3	HM3		
		Base metatarsal 3	BM3		
	Metatarsal 4	Head metatarsal 4	HM4		
		Base metatarsal 1	BM4		
	Metatarsal 5	Head of metatarsal 5	HM5	X	X
		Base metatarsal 5	BM5	X	X
Hallux	Proximal phalanx	Head of proximal phalanx 1	HLX		X
		Medial side of proximal phalanx 1	HLXM	X	

* Used to reconstruct markers proximal on the shank, which are outside the field of view of the scanner (Appendix C).
# OFM uses the marker in between the 2nd and 3rd metatarsal, which could not be placed because of the proximity to other markers, therefore HM2 is used instead in this study.

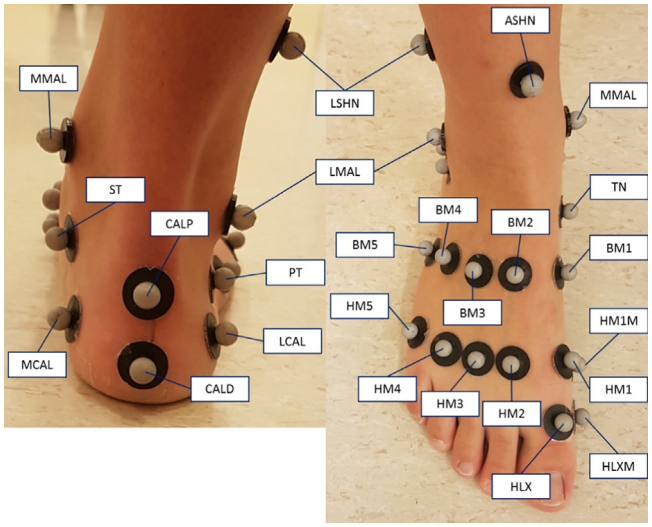

Fig. 1. Overview of marker placement. Abbreviations are explained in Table 1.

Fig. 2. Experimental setup with (A) the simulated weight-bearing device in the CT-scanner. Two examples of foot of foot plate positions: (B) medial view of the 20° dorsal flexion and (C) superior view of the 10° eversion.

Next, the difference vector was determined between the marker position in each loaded scan and in this reference scan. The norm of this vector was quantified as the 3D-displacement of the marker with respect to its underlying bone. In addition, this displacement was decomposed in the x, y and z components (x = anterior, y = proximal and z = lateral) of a marker-based CS of the whole foot, to assign generally accepted anatomical directions for these components (more details and results in Appendix B). This foot CS was defined in the neutral unloaded position according to the definitions of Cappozzo et al. (1995).

Second, the effect of marker displacements on the segment orientations as defined by OFM and RFM were quantified for every foot position for the shank, hindfoot and forefoot segments. The shank segment required one extra step to reconstruct markers outside of the scanning volume (Appendix C). Next, the STA vectors of all markers were transformed from the local bone CSs to the global CS. Subsequently, for every segment, two marker-based CSs were determined. The first CS was based on the marker positions from the reference scan in which no STAs were present (described by R_{ref}). The second CS was based on the marker positions after STAs of each marker were added to the reference position (described by $R_{withSTA}$). The rotation (R_{diff}) between the CSs with and without STAs included was determined for every foot position according to Eq. (1). R_{diff} matrices were decomposed according to (Grood and Suntay, 1983), which provided the error in segment orientation due to STAs in degrees for every foot position in the sagittal, frontal and transverse plane.

Table 2
Overview of CT-scans.

Scan	Footplate position	Scan abbreviation
1	Neutral (0°)*	NU
2	Neutral (0°)	NL
3	20° plantar flexion	20P
4	40° plantar flexion	40P
5	20° dorsal flexion	20D
6	10° eversion	10EV
7	10° inversion	10INV
8	Neutral (0°); Plate was pushed with forefoot only	TOE
9	Repetition of scan 4, 5 or 8#	40P2, 20D2 or TOE2
10	Repetition of scan 4, 5 or 8#	40P2, 20D2 or TOE2

* Unloaded (<10 N) with a tube charge of 50 mAs; other scans are loaded (70% body weight) with a 20 mAs tube charge.
# Each combination of two scans was appointed to five subjects randomly.

$$R_{diff} = inv(R_{ref}) * R_{withSTA} \quad (1)$$

Third, the effect of marker STAs on the joint angles as defined by OFM and RFM was quantified for the hindfoot-shank and forefoot-hindfoot joints. The reference joint angles were based on the segment CSs without STAs. For every scan, the 3D joint angles with STAs were determined based on the corresponding segment CSs with STAs. The differences between the joint angles with and without STA were considered as the error in joint angles due to STA in degrees (in three planes).

2.5. Statistics

Most marker displacements were normally distributed and therefore reported as mean and standard deviation over all subjects in each scan position. The errors in segment orientation and joint angles due to STAs were compared between models (i.e. OFM and RFM) and foot plate positions using 2-way repeated measures ANOVAs with marker model and foot plate position as factors. In case of significant effects ($p < 0.05$), post-hoc analyses with Bonferroni correction were performed. Statistical analyses were performed using Matlab and IBM SPSS statistical software (v.26, SPSS Inc., 192 Chicago, IL, USA).

3. Results

Displacements of each marker with respect to their underlying bone in every foot position are shown in Table 3. In general, largest marker displacements were shown when the foot was in 40° plantar flexion. The two markers with the largest 3D-displacement were on the lateral malleolus (LMAL) and proximally on the posterior aspect of the calcaneus (CALP). LMAL displaced considerably (>4mm) in all three directions (posterior, proximal and medial), while CALP mainly displaced distally (8.9 mm) with respect to the bone (Appendix B).

The effect of the marker displacement on the segment orientation is shown in Fig. 4. Significant interaction effects were present between the marker model and foot plate position in every plane of every segment ($p < 0.01$), hence separate paired t-tests were performed. The effect of STAs on the shank segment were < 1.5° in the sagittal and frontal plane. In the transverse plane, larger values were present, with average values up to 5.7° and individual values up to 10.9° in the 40° plantar flexion foot position. The effect of STAs on the hindfoot were mainly present in the sagittal and frontal plane. For RFM, largest values were shown in the sagittal plane when moving the foot plate in dorsal flexion (mean: 4.1°, max:

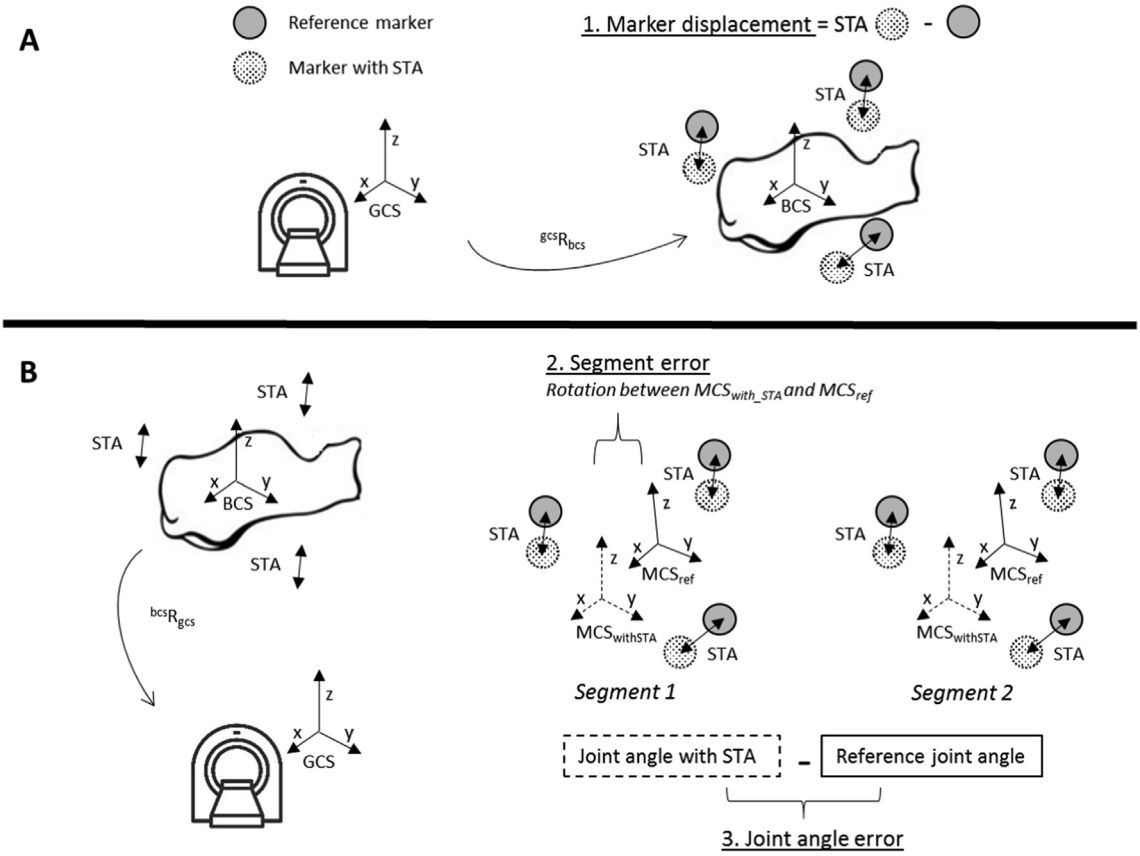

Fig. 3. Schematic overview of the data analysis to calculate (A) the 3D marker displacements (i.e. STAs) and (B) the error in segment orientation and joint angle due to STAs. Abbreviations: GCS: global coordinate system; BCS: bone coordinate system; ${}^{gcs}R_{bcs}$: rotation matrix from GCS to BCS; MCS_{ref}: marker coordinate system based on reference marker positions (solid). MCS_{with_STA}: marker coordinate system based on marker positions with STAs (dashed); ${}^{bcs}R_{gcs}$: rotation matrix from BCS to GCS.

Table 3
3D marker displacement in mm with respect to their underlying bone in different foot positions (mean ± SD).

Segment	Bone	Marker	Scanned foot positions						
			NL	20P	40P	20D	10EV	10INV	TOE
Shank	Tibia	MMAL	1.6±0.6	1.7±0.9	3.3±1.5	4.8±1.6	3.4±1.4	1.9±1.2	2.7±1.1
	Fibula	LMAL	2.8±1.4	9.2±3.6	11.5±4.0	4.4±2.0	5.2±2.6	3.5±2.3	8.1±2.6
Hindfoot	Calcaneus	CALD	1.3±0.5	1.6±0.7	2.0±0.8	1.4±0.8	1.6±1.0	1.3±1.0	1.8±1.2
		CALP	1.0±0.6	5.3±2.5	9.3±3.3	4.3±1.4	2.1±1.1	2.4±1.8	6.3±2.8
		MCAL	1.2±0.5	1.2±0.7	1.2±0.9	1.6±0.4	1.0±0.5	2.1±0.7	1.3±0.6
		LCAL	1.5±0.5	2.2±0.6	2.6±0.8	1.3±0.5	2.2±0.9	2.2±0.7	1.0±0.4
		PT	1.6±0.8	2.5±0.8	3.3±1.2	2.5±0.9	1.5±0.5	2.4±0.9	2.0±1.0
		ST	0.8±0.4	1.6±0.8	3.6±1.1	1.4±0.7	1.5±0.6	0.9±0.7	2.4±1.2
Midfoot	Navicular	TN	1.8±0.8	3.5±1.4	3.6±1.4	1.0±0.5	2.1±1.1	1.6±1.0	2.1±1.2
Forefoot	Metatarsal 1	HM1	1.0±0.7	0.8±0.4	1.2±0.6	1.1±0.5	1.9±0.9	1.1±0.7	2.5±1.4
		HM1M	2.2±0.8	2.1±0.9	2.2±1.0	2.5±1.0	2.3±1.0	3.0±1.5	3.5±1.9
		BM1	0.7±0.3	1.1±0.4	2.2±0.9	1.0±0.5	0.9±0.4	0.8±0.5	1.5±0.9
	Metatarsal 2	HM2	1.9±0.5	1.5±0.6	1.0±0.4	1.9±0.5	1.6±0.7	2.0±0.6	2.5±1.5
		BM2	1.5±0.5	1.4±0.6	3.7±1.4	2.0±0.5	1.0±0.5	1.9±0.5	1.6±1.1
	Metatarsal 3	HM3	2.1±0.7	1.6±0.7	1.3±0.7	2.2±0.7	1.6±1.0	2.4±0.8	1.9±1.2
		BM3	1.6±0.5	0.9±0.4	3.2±1.3	2.2±0.4	1.1±0.6	2.0±0.6	1.5±1.1
	Metatarsal 4	HM4	1.9±0.6	1.8±0.8	1.4±0.7	2.0±0.5	1.5±0.8	2.6±0.9	2.0±1.0
		BM4	1.3±0.6	0.9±0.5	2.3±1.1	1.6±0.6	1.1±0.7	1.8±0.8	1.5±0.9
	Metatarsal 5	HM5	1.2±0.5	1.4±0.7	1.7±0.8	1.5±0.7	1.8±1.2	3.2±1.5	2.6±1.1
		BM5	1.1±0.6	1.7±0.7	2.4±0.7	1.0±0.7	1.3±0.7	2.3±1.1	1.2±0.7
Hallux	Proximal phalanx	HLX	0.8±0.5	0.7±0.6	0.9±0.7	1.0±0.6	1.0±0.6	1.1±0.5	1.1±0.6
		HLXM	1.1±0.9	1.5±1.1	1.8±1.3	1.5±1.1	1.3±0.6	1.9±1.2	1.6±1.3

Note: Marker and scan abbreviations are explained in Table 1 and 2

Color coding: linear distribution from lowest (white) to highest (red) value

6.8°) or 40° plantar flexion (mean: 5.7°, max: 10.3°). For OFM the largest values were present when moving the foot in inversion (mean: 3.5°, max: 5.6°). The effect of STAs on the forefoot were relatively small in all planes (< 2.1°).

The effect of marker displacement on the joint angles is shown in Fig. 5. Interaction effects between marker model and foot plate position were present in every plane for both joint angles ($p < 0.01$). When loading the foot, all joint angles were affected < 1.3° by marker displacements, except the transverse plane angle of HF-SK (mean: 2.3°). Largest values were shown for HF-SK in 40° plantar flexion). For RFM, the sagittal plane was most affected (mean: 6.7°, max: 11.8°). For OFM, the highest value was shown in the transverse plane (mean: 3.9°, max: 6.8°), however this value was not significantly different from RFM. When the foot plate was positioned into inversion and eversion, largest errors were shown in the frontal plane for OFM joint angles and the transverse plane for RFM joint angles. FF-HF angles were most affected by STAs in the sagittal plane for RFM (mean: 4.5°, max: 11.0°) and in the frontal plane for OFM (mean: 2.4°, max: 5.8°).

4. Discussion

This study quantified the soft tissue artifacts of skin-mounted markers on the foot and their effect on segment and joint angles in 3D as defined by the Oxford and Rizzoli Foot Models. Largest displacement values were found for the markers proximally on the posterior aspect of the calcaneus (CALP, 9.3 mm) and the lateral malleolus (LMAL, 11.5 mm). It was shown that STAs affect multi-segment foot kinematics with joint angle errors up to 6.7° on average over the subjects and maximal individual values up to 11.8° when the footplate was positioned in 40° plantar flexion. RFM was most affected in the sagittal plane for the joints around the hindfoot and OFM was most affected in the other two planes for the hindfoot-shank angle, but to a lesser extent.

This study was the first to quantify STAs (i.e. 3D-displacements) of all foot markers used in the two most commonly-used multi-segment foot models. Of all markers, the CALP and LMAL markers showed the largest displacement with respect to the underlying bone (9.3 mm and 11.5 mm). To our knowledge, no literature into STAs of the CALP marker is available, but large STA values have been reported previously for the LMAL marker (15 mm) when the foot was fully supinated (Birch and Deschamps, 2011). High values (16 mm) have also been shown for the navicular marker (Shultz et al., 2011), while only relatively small values were shown in our study (40P position: 3.6 ± 1.4 mm). The high values in the previous study might be caused by the use of marker triads, since other studies without marker triads reported values closer to ours (2.0–4.5 mm) (Maslen and Ackland, 1994; Tranberg and Karlsson, 1998). Three main factors cause STAs (Okita et al., 2009): (I) skin deformation, II) bone motion beneath the skin and (III) dynamic effects (e.g. inertia of the markers during impact). The first two fac-

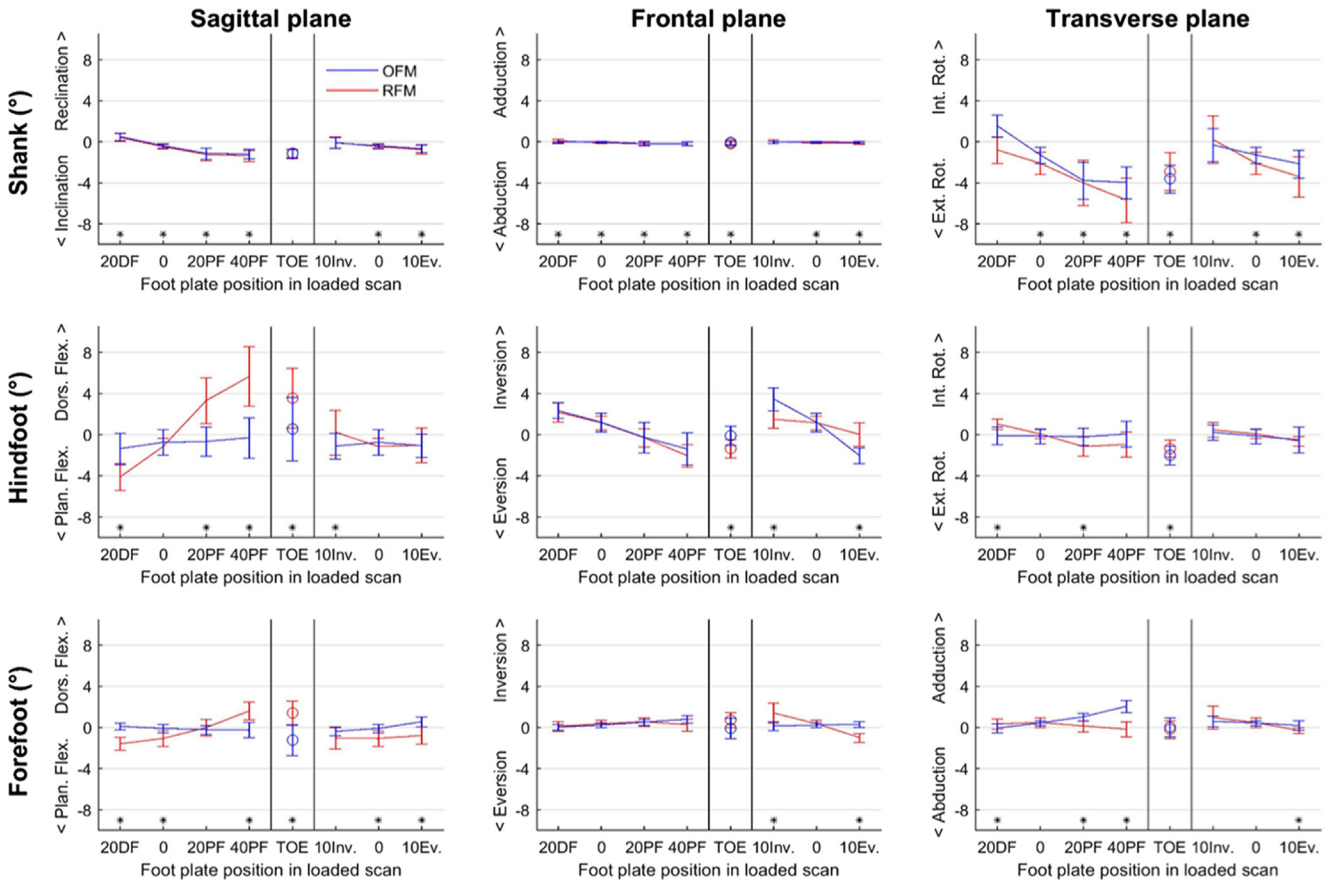

Fig. 4. The effect of STAs on the shank-, hindfoot- and forefoot segment orientations for the Oxford Foot Model (OFM) (blue) and the Rizzoli Foot Model (RFM) (red) in the different loaded foot plate positions in three planes. Clinical terminology is used on the vertical axes titles of the graphs to describe the rotations of the different segments in the same plane. *Indicates that OFM and RFM results are significantly different. Abbreviations are explained in Table 2. (For interpretation of the references to colour in this figure legend, the reader is referred to the web version of this article.)

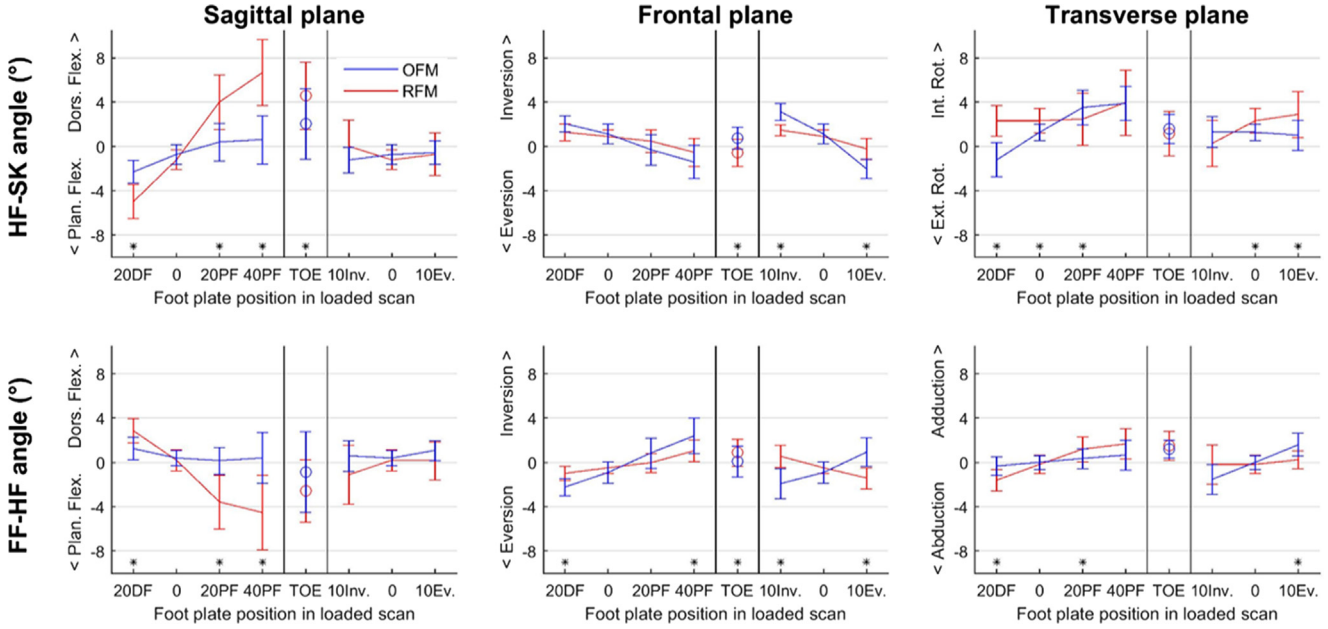

Fig. 5. The effect of STAs of the hindfoot-shank (HF-SK) and forefoot-hindfoot (FF-HF) joint angle for the Oxford Foot Model (OFM) (blue) and the Rizzoli Foot Model (RFM) (red) in the different loaded foot plate positions in three planes. Clinical terminology is used on the vertical axes titles of the graphs to describe the rotations of the different segments in the same plane. *Indicates that OFM and RFM results are significantly different. Abbreviations are explained in Table 2. (For interpretation of the references to colour in this figure legend, the reader is referred to the web version of this article.)

tors probably cause the large STAs of the CALP and LMAL markers. The CALP marker is placed on the skin above the Achilles tendon attachment to the calcaneus, when the foot moves the skin shrinks or stretches and the marker is probably following the tendon movement more than the calcaneal movement. The LMAL marker is likely displaced as a result of the malleolar shape and thin skin around it resulting in sliding of the skin around the malleolus. The second factor also plays a role in the STAs found for the forefoot markers. These markers have relatively small STAs, which seem to be mainly caused by loading instead of moving the foot, since the values of the neutral loaded scan are similar to the scans in which the foot is also positioned differently. During loading, the metatarsals probably move more towards the ground and therewith further away from the marker. The third factor (i.e. dynamic effects) was not included in the present study, because the measurement were performed in static positions. During normal walking, dynamic effects will likely be present and are expected to add an extra error to the STAs.

STAs of the markers caused errors in the kinematic output of the foot models. The shank orientation of both models, was mainly affected by STAs in the transverse plane, but barely in the other two planes, despite the large errors in LMAL. This is probably a result of the distance between LMAL and the marker proximal on the tibia, which was about 7 times larger than the distance between the malleoli markers. With a large distance between markers, an error in marker position has less effect on the angle of its direction compared to when markers are close to each other. For the hindfoot segment CS, the sagittal plane of RFM was most affected by STAs, whereas OFM did not show large errors in that plane. This is due to the fact that CALP is used differently in the models' definitions (Schallig et al., 2020). In RFM, CALP is used as a tracking marker and origin of the hindfoot CS, while OFM does not use it as a tracking marker but just to define the anatomical CS. Hence, STA of the CALP marker does influence RFM but not the OFM kinematics.

The effect of STAs on the hindfoot-shank angle in the sagittal plane of RFM is the largest joint angle error reported. The relatively large effect of STAs on the hindfoot orientation and the smaller effect on shank orientation were in opposite directions, which means that the hindfoot was measured in more dorsal flexion, while the shank was inclined as a result of the marker displacement. Therefore, the errors in those segment orientations due to STAs added up. The contrary occurs for the forefoot-hindfoot error, in which the hindfoot and forefoot errors due to STAs are in the same direction and therefore cancel each other out. In general, STAs of the forefoot markers and their effect on the forefoot CS and corresponding joint angles is minor. Even in the TOE position the errors due to STAs were small, although more skin deformation could have been expected affecting the markers at the forefoot.

Several limitations need to be taken into account when interpreting the results of this study. First, the participants of this study were healthy volunteers. Therefore, these results cannot directly be applied to patients, who for example might have bony deformities. However, this study still highlights the markers that are vulnerable to STAs. The actual absolute STA values will likely also depend on foot size and the amount of soft tissue covering the bones of the foot. Second, the effect of STAs on kinematics was only determined for OFM and RFM, while a lot of other multi-segment foot models are available (Leardini et al., 2019). However, the effect of STAs on joint angles as calculated in other models can also be determined with the data presented in this study (Appendix B). Third, our experimental setup has not been used previously for the purpose of quantifying STAs and therefore the measurement errors are unknown. However, our repeatability analysis (Appendix A) showed a good repeatability,

The large STAs shown in this study have clinical implications. Generally in gait analysis, an angular difference of >5° is considered clinically relevant (McGinley et al., 2009). Our study shows that in extreme foot positions STAs affect the joint angles on average 6.7°, which means that clinically relevant errors due to STAs can occur. Moreover, large individual differences in STAs between subjects are present, as shown by the large standard deviations in this study and also mentioned by others (Maslen and Ackland, 1994; Reinschmidt et al., 1997; Shultz et al., 2011). These standard deviations are larger in extreme foot positions with large STAs. The inter-subject variance in bone morphology and in thickness and elastic properties of tissues in between bone and marker might be more evident in these foot positions. However, More research is needed to identify what exactly causes the change in variability and if a relation exists with particular patient characteristics. Because of the large average STA values and inter-subject differences, it is advised to make adaptations to the model definitions to minimize STA errors and to assure that the models can still be used in a clinical setting. The use of markers such as CALP and LMAL as tracking markers in the models should be reconsidered.

5. Conclusion

This study showed that soft tissue artifacts introduce clinically relevant errors in multi-segment foot model kinematics. Joint angles were most affected by soft tissue artifacts in the sagittal plane for RFM and the other two planes for OFM. Especially STAs of markers proximally on the posterior aspect of the calcaneus and the lateral malleolus are sources of error and should therefore not be used as tracking markers.

Declaration of Competing Interest

The authors declare that they have no known competing financial interests or personal relationships that could have appeared to influence the work reported in this paper.

Supplementary material

Supplementary data to this article can be found online at https://doi.org/10.1016/j.jbiomech.2021.110359.

References

Birch, I., Deschamps, K., 2011. Quantification of skin marker movement at the malleoli and talar heads. J. Am. Podiatr. Med. Assoc. 101, 497–504.
Cappozzo, A., Catani, F., Croce, U.D., Leardini, A., 1995. Position and orientation in space of bones during movement: anatomical frame definition and determination. Clin. Biomech. (Bristol, Avon) 10, 171–178.
Chen, S.J., Mukul, M., Chou, L.S., 2011. Soft-tissue movement at the foot during the stance phase of walking. J. Am. Podiatr. Med. Assoc. 101, 25–34.
Dobbe, J.G.G., de Roo, M.G.A., Visschers, J.C., Strackee, S.D., Streekstra, G.J., 2019. Evaluation of a quantitative method for carpal motion analysis using clinical 3-D and 4-D CT protocols. IEEE Trans. Med. Imaging 38, 1048–1057.
Grood, E.S., Suntay, W.J., 1983. A joint coordinate system for the clinical description of three-dimensional motions: application to the knee. J. Biomech. Eng. 105, 136–144.
Kang, D.H., Kang, C., Hwang, D.S., Song, J.H., Song, S.H., 2017. The value of axial loading three dimensional (3D) CT as a substitute for full weightbearing (standing) 3D CT: Comparison of reproducibility according to degree of load. Foot Ankle Surg.
Kessler, S.E., Rainbow, M.J., Lichtwark, G.A., Cresswell, A.G., D'Andrea, S.E., Konow, N., Kelly, L.A., 2019. A direct comparison of biplanar videoradiography and optical motion capture for foot and ankle kinematics. Front. Bioeng. Biotechnol. 7, 199.
Kleipool, R.P., Dahmen, J., Vuurberg, G., Oostra, R.J., Blankevoort, L., Knupp, M., Stufkens, S.A.S., 2019. Study on the three-dimensional orientation of the posterior facet of the subtalar joint using simulated weight-bearing CT. J. Orthop. Res. 37, 197–204.
Leardini, A., Benedetti, M.G., Berti, L., Bettinelli, D., Nativo, R., Giannini, S., 2007. Rear-foot, mid-foot and fore-foot motion during the stance phase of gait. Gait Posture 25, 453–462.

Leardini, A., Caravaggi, P., Theologis, T., Stebbins, J., 2019. Multi-segment foot models and their use in clinical populations. Gait Posture 69, 50–59.
Leardini, A., Chiari, L., Della Croce, U., Cappozzo, A., 2005. Human movement analysis using stereophotogrammetry. Part 3. Soft tissue artifact assessment and compensation. Gait Posture 21, 212–225.
Maiwald, C., Arndt, A., Nester, C., Jones, R., Lundberg, A., Wolf, P., 2017. The effect of intracortical bone pin application on kinetics and tibiocalcaneal kinematics of walking gait. Gait Posture 52, 129–134.
Maslen, B.A., Ackland, T.R., 1994. Radiographic study of skin displacement errors in the foot and ankle during standing. Clin. Biomech. (Bristol, Avon) 9, 291–296.
McGinley, J.L., Baker, R., Wolfe, R., Morris, M.E., 2009. The reliability of three-dimensional kinematic gait measurements: a systematic review. Gait Posture 29, 360–369.
Nester, C., Jones, R.K., Liu, A., Howard, D., Lundberg, A., Arndt, A., Lundgren, P., Stacoff, A., Wolf, P., 2007. Foot kinematics during walking measured using bone and surface mounted markers. J. Biomech. 40, 3412–3423.
Okita, N., Meyers, S.A., Challis, J.H., Sharkey, N.A., 2009. An objective evaluation of a segmented foot model. Gait Posture 30, 27–34.
Portinaro, N., Leardini, A., Panou, A., Monzani, V., Caravaggi, P., 2014. Modifying the Rizzoli foot model to improve the diagnosis of pes-planus: application to kinematics of feet in teenagers. J. Foot Ankle Res. 7, 57.
Ramsey, D.K., Wretenberg, P.F., Benoit, D.L., Lamontagne, M., Nemeth, G., 2003. Methodological concerns using intra-cortical pins to measure tibiofemoral kinematics. Knee Surg. Sports Traumatol. Arthrosc. 11, 344–349.
Reinschmidt, C., van Den Bogert, A.J., Murphy, N., Lundberg, A., Nigg, B.M., 1997. Tibiocalcaneal motion during running, measured with external and bone markers. Clin. Biomech. (Bristol, Avon) 12, 8–16.
Rodda, J.M., Graham, H.K., Carson, L., Galea, M.P., Wolfe, R., 2004. Sagittal gait patterns in spastic diplegia. J. Bone Joint Surg. Br. 86, 251–258.
Schallig, W., van den Noort, J.C., Kleipool, R.P., Dobbe, J.G.G., van der Krogt, M.M., Harlaar, J., Maas, M., Streekstra, G.J., 2019. Precision of determining bone pose and marker position in the foot and lower leg from computed tomography scans: How low can we go in radiation dose?. Med. Eng. Phys. 69, 147–152.
Schallig, W., van den Noort, J.C., McCahill, J., Stebbins, J., Leardini, A., Maas, M., Harlaar, J., van der Krogt, M.M., 2020. Comparing the kinematic output of the Oxford and Rizzoli Foot Models during normal gait and voluntary pathological gait in healthy adults. Gait Posture 82, 126–132.
Shultz, R., Kedgley, A.E., Jenkyn, T.R., 2011. Quantifying skin motion artifact error of the hindfoot and forefoot marker clusters with the optical tracking of a multi-segment foot model using single-plane fluoroscopy. Gait Posture 34, 44–48.
Stebbins, J., Harrington, M., Thompson, N., Zavatsky, A., Theologis, T., 2006. Repeatability of a model for measuring multi-segment foot kinematics in children. Gait Posture 23, 401–410.
Tranberg, R., Karlsson, D., 1998. The relative skin movement of the foot: a 2-D roentgen photogrammetry study. Clin. Biomech. (Bristol, Avon) 13, 71–76.
Westblad, P., Hashimoto, T., Winson, I., Lundberg, A., Arndt, A., 2002. Differences in ankle-joint complex motion during the stance phase of walking as measured by superficial and bone-anchored markers. Foot Ankle Int. 23, 856–863.